

# Magnetotransport properties of a single grain boundary in a bulk La–Ca–Mn–O material

B. Vertruyen, R. Cloots,<sup>a)</sup> and A. Rulmont  
*SUPRAS and LCIS, Chemistry Institute B6, Sart Tilman, University of Liège, B-4000 Liège, Belgium*

G. Dhalenne  
*Laboratoire de Physico-Chimie de l'Etat Solide, Université Paris-Sud, 91405 Cédex Orsay, France*

M. Ausloos  
*SUPRAS, Physics Institute B5, Sart-Tilman, University of Liège, B-4000 Liège, Belgium*

Ph. Vanderbemden  
*SUPRAS and MIEL, Montefiore Institute B28, Sart Tilman, University of Liège, B-4000 Liège, Belgium*

(Received 16 July 2001; accepted for publication 17 August 2001)

Besides the “intrinsic” colossal magnetoresistance effect observed in single crystals, the polycrystalline manganate compounds also exhibit an “extrinsic” magnetoresistance related to the presence of grain boundaries. We report electrical transport and magnetic measurements carried out on a bigrain sample extracted from a floating zone method-grown rod of calcium doped lanthanum manganate. Electrical resistance was measured both within a grain and across the grain boundary, between 20 and 300 K and from 0 to 8 T. Magnetoresistance values up to 99% are reached within the grain. The temperature dependence of the resistance across the grain boundary displays a “foot-like” feature towards the bottom of the transition. Low field and high field magnetoresistance effects are examined. We compare our results for a “bulk” grain boundary to those obtained by other authors for bicrystal thin films and bulk polycrystalline materials. © 2001 American Institute of Physics. [DOI: 10.1063/1.1410885]

## I. INTRODUCTION

The  $\text{Ln}_{1-x}\text{A}_x\text{MnO}_{3\pm d}$  family (where Ln is a large lanthanide and A generally an alkaline-earth) was extensively studied during the early 1990s.<sup>1</sup> These perovskites had already been characterized in the 1950s,<sup>2,3</sup> but the interest was renewed by the discovery of colossal magnetoresistance (CMR)<sup>4</sup> properties in some of these materials: the electrical resistance drastically decreases by application of a magnetic field. The magnetoresistance is defined as  $(R_0 - R_H)/R_0$ , where  $R_H$  and  $R_0$  denote the resistance with and without magnetic field, respectively.

These compounds crystallize in the perovskite structure  $\text{ABO}_3$ , where the A site is defined by eight corner-sharing  $\text{BO}_6$  octahedra. The ideal structure is easily distorted in order to accommodate cations of different sizes. The  $\text{LnMnO}_3$  parent compounds can be doped either on the lanthanide or on the manganese sites, yielding extended solid solutions.<sup>5</sup> Only a few compounds display CMR properties. The simple phenomenological model of double exchange,<sup>6</sup> which qualitatively explains the CMR phenomenon, turned out to be unable to account for the amazing diversity of behaviors that can be observed throughout that family. Many parameters appear to influence the physical properties of those materials. The two most meaningful ones are the  $\text{Mn}^{4+}/\text{Mn}^{3+}$  ratio (= the charge carrier density) and the local crystallographic structure of the Mn–O network (which influences the orbital overlapping between adjacent manganese ions).<sup>5</sup>

Beside those intrinsic parameters, it turns out that the microstructure of the material can have a strong influence on the physical properties, as proved by comparative studies of thin films, bulk ceramics, and single crystals.<sup>7–9</sup> On one hand, the magnetoresistance of single crystals and epitaxial thin films is quite large but concentrated within a temperature range around the transition temperature  $T_C$ . On the other hand, polycrystalline materials, either bulk ceramics or thin films, display a significant magnetoresistance at low fields and all temperature below  $T_C$ . Due to the small size of the grains usually found in bulk polycrystalline materials, it is generally impossible to isolate the behavior of grain boundaries. Therefore the physical properties are frequently reported as a function of the grain size which can be tuned by modifying the synthesis conditions.<sup>10–12</sup> Most of the systematic investigations devoted to individual grain boundaries have thus been carried out in thin films. By growing epitaxial thin films on bicrystal substrates,<sup>13–18</sup> well-controlled grain boundaries can be obtained. For example, Evetts *et al.*<sup>18</sup> have studied films patterned in such a way that only the contribution of the grain boundary to the resistance is measured. But although thin films studies allow for an efficient control of the grain boundary misorientation, it is not clear whether the boundaries in films and those in bulk materials should behave in a similar manner. In addition, the film substrate is likely to influence the electrical properties by introducing crystallographic strains which are expected to be modulated<sup>19,20</sup> in the vicinity of the interface.

Therefore in this article, we report electrical and magnetic measurements carried out on a single grain boundary of

<sup>a)</sup>Electronic mail: rcloots@ulg.ac.be

a bulk CMR material. This allows us to bring out the genuine boundary behavior without any substrate effects. We will contrast the properties of such a boundary with those found in bicrystal thin films and polycrystalline materials. Moreover, we show how large a change in resistivity can be in such materials.

## II. EXPERIMENT

### A. Synthesis process

A 30-mm long 4-mm diameter cylindrical rod consisting of large ( $\sim 1 \text{ mm}^3$ ) calcium-doped lanthanum manganate (LCMO) grains was grown by the floating zone method.  $\text{La}_2\text{O}_3$ ,  $\text{CaCO}_3$ , and  $\text{MnO}_2$  of high purity were used as starting materials. Hygroscopic  $\text{La}_2\text{O}_3$  was calcined for dehydration before use. Polycrystalline  $\text{La}_{0.7}\text{Ca}_{0.3}\text{MnO}_3$  powder was prepared by the standard solid state reaction. The quality of the material was checked by x-ray diffraction. A feed rod was then pressed isostatically at about 1800 bar and sintered at  $1300^\circ\text{C}$ . The pressing–sintering cycle was repeated several times in order to achieve a high density of the feed rod. The rod was grown in a NEC image furnace under flowing  $\text{O}_2$  at a crystallization rate of about 2 mm/h. The (polycrystalline) seed rod and the feed rod were rotated in opposite directions in order to homogenize the molten zone. No subsequent annealing was carried out. Sections were cut from both ends of the rod, put into resin, and polished for microstructural analysis. Optical microscopy with polarized light (Olympus AH3-UMA) revealed the polycrystalline nature of the rod. However, the far end of the rod is made up of only a few grains. Energy dispersive x-ray (EDX) analysis (Oxford Link Pentafet) did not show any secondary phase. However, the chemical composition was found to vary slightly along the rod longitudinal axis. This was expected because of the manganese vaporization during the growth and the low value of the calcium distribution coefficient between solid and liquid phases.<sup>21</sup> On the contrary, the chemical composition throughout a transversal section of the rod was found to be homogeneous within the uncertainty of the EDX method.

A 0.5-mm thick slice of the far end of the rod was cut and both faces were polished. Optical micrographies in polarized light of both faces (Fig. 1) showed the presence of only three large grains. Bar-shaped samples of typical size  $0.15 \times 0.8 \times 0.8 \text{ mm}^3$  were carefully excised from the rod sample using a wire saw. Each specimen contained either a single grain or two adjacent grains with the boundary approximately perpendicular to the length of the bar. The grain boundary structure was visible on the largest faces of the bar after polishing.

From EDX analysis, the cationic composition of the measured samples turned out to be  $\text{La}_{0.78}\text{Ca}_{0.22}\text{Mn}_{0.9}\text{O}_x$ . The knowledge of the density (measured by the Archimedes' method) and the cell volume (refined from XRD data in the  $Pbnm$  space group, with the FULLPROF software) enabled us to calculate the molar mass. The oxygen content could thus be estimated, yielding a chemical composition close to  $\text{La}_{0.78}\text{Ca}_{0.22}\text{Mn}_{0.9}\text{O}_{2.94}$ . The theoretical number of Bohr magnetons estimated for such a chemical content ( $3.20 \mu_B$ ) is in

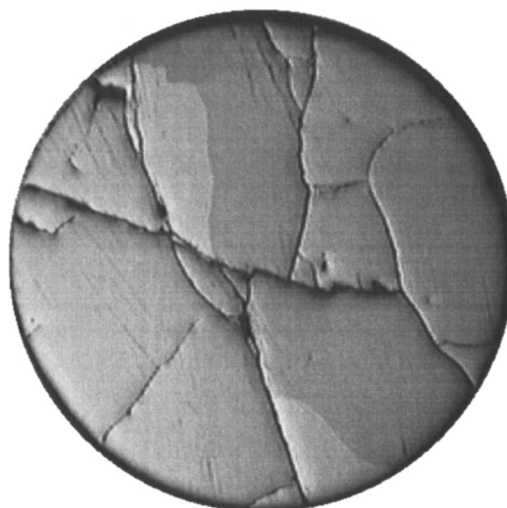


FIG. 1. Optical micrograph with polarized light: transversal section in the rod.

good agreement with the experimental value of  $3.17 \mu_B$  determined by measuring the saturation magnetization at  $T = 50 \text{ K}$  and  $\mu_0 H = 5 \text{ T}$ .

### B. Physical measurements

Very small electrical contacts were achieved by attaching thin gold wires ( $33 \mu\text{m}$  diameter) to the samples using DuPont 6838 silver epoxy paste annealed in flowing  $\text{O}_2$  for 5 min. In samples containing grain boundaries, voltage contacts were placed both within the grain and across the well-defined grain boundary, as sketched in Fig. 2. Resistance and magnetoresistance measurements were carried out using the conventional four-point technique. The data were acquired as a function of magnetic field and temperature using a Quantum Design PPMS. Before each measuring sequence the remnant field of the superconducting magnet was eliminated by the standard practice of applying a succession of decreasing fields in alternate directions. For all measurements discussed below the influence of increasing and decreasing temperatures was examined, but no hysteresis was noticed within the temperature measurement accuracy (0.1 K). dc magnetization measurements at several temperatures were carried out. Three samples were characterized in order to confirm the reproducibility of the results. Apart from some minor variations of  $T_C$ , all general electrical characteristics were the same. Therefore the following discussion concentrates on the behavior of one of those samples.

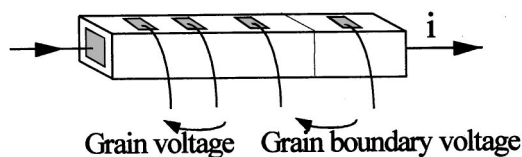


FIG. 2. Sketch of the electrical contacts.

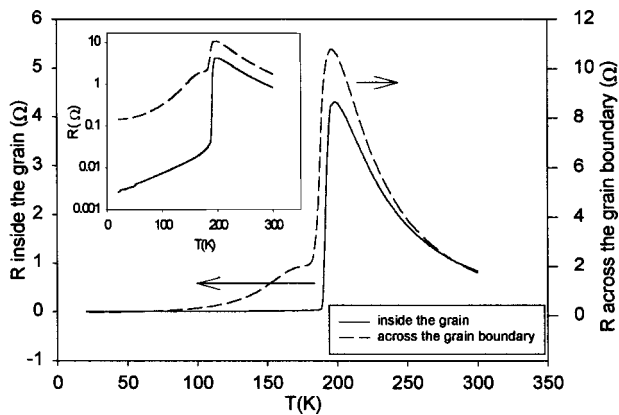


FIG. 3. Temperature dependence of the resistance inside the grain and across the grain boundary. Inset: same data with logarithmic scale for the resistance.

### III. RESULTS AND DISCUSSION

#### A. Electrical resistance in zero field

Figure 3 displays a recording of the electrical resistance versus temperature curves measured within a grain and across the grain boundary, respectively. In the inset, the same data are plotted on a logarithmic scale. The resistive transition of the grain is observed to be very sharp, without any intermediate step. The resistance drop is greater than two orders of magnitude. On the other hand, the resistance across the grain boundary decreases sharply at the transition temperature before levelling off to form a “foot-like” structure towards the bottom of the transition at lower temperature. The strong initial decrease is caused by the grain so-called metal–insulator transition whereas the broader feature can be clearly attributed to the existence of the grain boundary.

Before discussing these results, it is worth emphasizing that the striking difference in the resistivity behavior inside the grain and across the grain boundary do confirm, *a posteriori*, that no unseen grain boundary is present in our claimed “grain.” It can also be noticed that the transition temperatures, defined as the position of the maxima in the  $R(T)$  curves, are slightly different for the data measured within the single grain and across the grain boundary (198.7 and 196.0 K, respectively). This small  $T_C$  difference is likely to be related to the individual properties of the two grains since a very little difference in the chemical composition of the two grains (not detected during the chemical characterization) cannot be ruled out.

We will first deal with the high-temperature regime (230–300 K). In that temperature range both curves can be well fitted by a classical activation energy law:

$$\rho = \rho_{\infty} \exp\left(\frac{E_0}{kT}\right).$$

The values for the gap  $E_0$  obtained by fitting the experimental data are 0.096 and 0.103 eV for the resistance within the grain and across the grain boundary, respectively, in very good agreement with the typical value of 0.1 eV reported by other authors.<sup>1</sup>

Next, we turn to the low-temperature regime ( $T < T_C$ ). As can be seen from the inset of Fig. 3, the resistance across the boundary is at least two orders of magnitude higher than the grain resistance itself. More precisely, the low-temperature dependence of the resistance across the grain boundary can be viewed as a large bump superimposed to the main peak characteristic of the grain transition. Therefore it would be tempting to perform a numerical deconvolution and use the grain data for extracting the temperature dependence of the boundary contribution to the resistance. Attempts to do so did not give satisfactory results because (i) the transition temperatures are slightly different, and (ii) the system is expected to be more complicated than resistances placed in series, i.e., the current may flow across the boundary through some percolation paths corresponding to the best coupled neighboring regions.<sup>22</sup> Nevertheless, at temperatures just below  $T_C$  (i.e.,  $160 \text{ K} < T < 180 \text{ K}$ ), the boundary is seen to be far more resistive than the grain. We can thus consider the bump in the measured resistance to be due exclusively to the boundary and, within a reasonable accuracy, estimate the value of the so-called specific boundary resistivity  $\rho_B \cdot d$ , where  $d$  is the distance between the voltage contacts. In this temperature range we find  $\rho_B \cdot d \sim 10^{-7} \Omega \text{ cm}^2$ . This value is similar to those determined on an artificial grain boundary obtained by growing an epitaxial thin film on a bicrystal substrate for a similar compound.<sup>23</sup> In comparing the behavior of thin films and bulk boundaries, the unusual feature of the data displayed in Fig. 3 is the well-defined “plateau” below  $T_C$ . In polycrystalline pellets or films, a rather large broadening of the resistance peak is generally observed instead of a shoulder.<sup>10</sup> This can be explained by the distribution of transition temperature resulting from a large number of slightly different grains together with a variety of grain boundaries. In our case, the presence of the shoulder in the resistance curve is clearly the signature of the single grain boundary.

#### B. Temperature dependence of the magnetoresistance

The influence of applied magnetic fields ranging from 0.5 to 8 T on the electrical resistance was investigated. As usual in those materials, the resistance peaks are shifted towards higher temperatures with increasing magnetic field. The same feature (not shown here) was observed. Figure 4 shows the magnetoresistance  $[R(B) - R(B=0)]/R(B=0)$  within the grain as a function of temperature. The magnetoresistance within the grain is concentrated around the transition temperature, where it reaches the remarkable peak values of 98.3% under 1 T, corresponding to a two orders of magnitude decrease in resistance. Since the magnetoresistance cannot exceed 100%, the magnetoresistive response inevitably saturates (MR under 8 T = 99.3%). However, the temperature range of the CMR effect increases with increasing magnetic field.

The magnetoresistance across the grain boundary is shown in Fig. 5. The magnetoresistance at the main peak reaches only 74.3% under 1 T (to be compared to 98.3% inside the grain). Larger fields are necessary to achieve very high CMR values (96.2% under 8 T). The presence of the

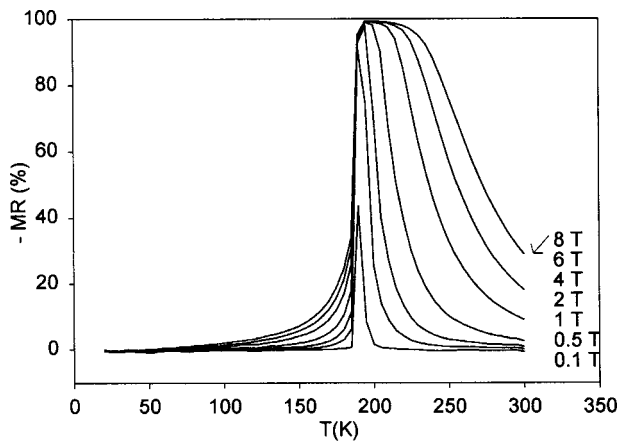


FIG. 4. Temperature dependence of the magnetoresistance (MR) inside the grain for magnetic fields as indicated.

grain boundary appears to require much higher fields than 1 T for the “saturation magnetoresistance” to be obtained. Besides, the magnetoresistance across the grain boundary displays two additional features: (i) a bump corresponding to the shoulder in the resistance curve and (ii) a nonvanishing low-temperature magnetoresistance. Since these peculiarities are not visible for the grain, they are thus related to the presence of the grain boundary. The magnetoresistance at the bump reaches very high values under high fields: 85.8% under 8 T. However, the magnetoresistance under 1 T is only 25.2%: although the grain boundary magnetoresistance is generally considered to be a low-field effect, here the high-field component is highly significant.

**C.  $R(H)$  curves at several temperatures**

Figure 6 shows the field dependence of the resistance ( $-1\text{ T} < \mu_0 H < 1\text{ T}$ ) measured at several fixed temperatures below and above  $T_C$ . First we examine the grain behavior [Fig. 6(a)]. As expected, a magnetoresistance is only observed near the transition temperature. The magnetic field promotes ferromagnetic order by compensating the thermal disorder: the resistivity is drastically reduced, yielding the CMR effect. The same mechanism accounts for the field de-

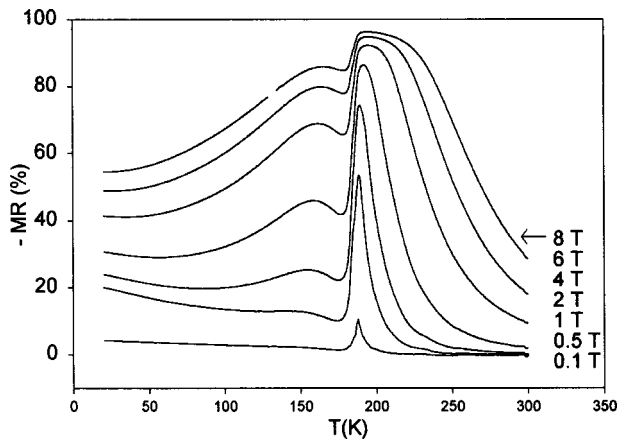


FIG. 5. Temperature dependence of the magnetoresistance (MR) across the grain boundary for magnetic fields as indicated.

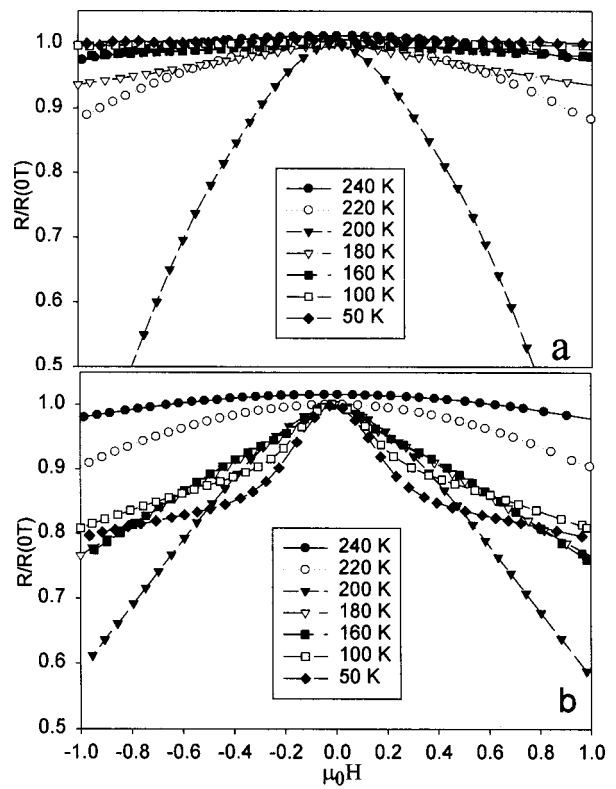


FIG. 6. Field dependence of the resistance (a) within the grain and (b) across the grain boundary.

pendence of the resistance across the grain boundary at and above 200 K. However, at 200 K the field dependence is weaker than within the grain because the grain boundary remains insulating. The grain resistance versus field curves display a parabolic behavior around  $T_C$ . Since we measured both the resistance and the magnetic moment (Fig. 7) as a function of the applied field, we could apply the scaling expression given by Inoue and Maekawa<sup>24</sup>

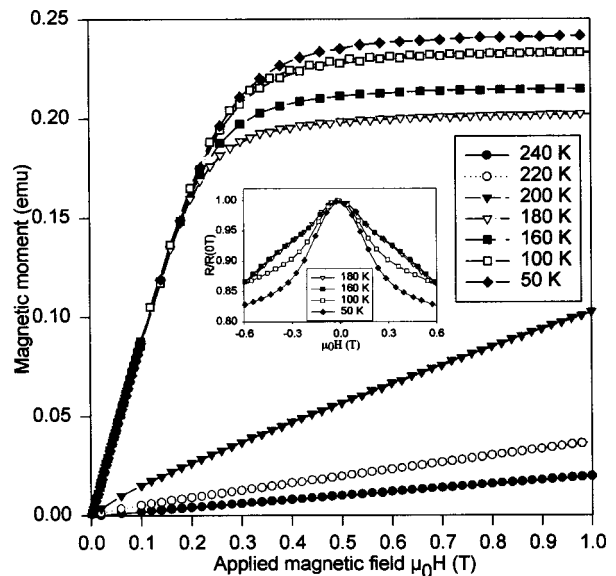


FIG. 7. Field dependence of the bigrain magnetic moment. Inset: Field dependence of the resistance across the grain boundary between  $-0.6$  and  $0.6\text{ T}$ .

$\rho = \rho_0 \{1 - C(M/M_S)^2\}$ , where  $M_S$  is the saturation magnetization. Theoretically this model is valid only near the transition temperature, when the interactions between spins are still weak. This is indeed what we observe, as could be expected from the parabola-like behaviors of the field dependences of the resistance near the transition temperature. We correlate the resistance data inside the grain with the overall magnetization which is more representative of the property of the major volume fraction. This fit yields a  $C$  value of about 4.5, in good agreement with the value of Akther Hossain *et al.*<sup>11</sup> for polycrystalline  $\text{La}_{0.7}\text{Ca}_{0.3}\text{MnO}_3$  pellets ( $C=4.6$ ). This value is noticeably higher than those calculated by Fukurawa<sup>25</sup> for the  $\text{La}_{1-x}\text{Sr}_x\text{MnO}_3$  system. This is not surprising, because the coefficient  $C$  is related to the ratio  $J/W$  (where  $J$  is the Hund coupling and  $W$  the electronic bandwidth) and  $W$  is smaller in the  $\text{La}_{1-x}\text{Ca}_x\text{MnO}_3$  system than in the  $\text{La}_{1-x}\text{Sr}_x\text{MnO}_3$  system.

Next we examine the field dependence of the resistance measured across the grain boundary [Fig. 6(b)]. The magnetoresistance across the grain boundary does not vanish at lower temperatures, unlike the grain behavior. Above the transition temperature ( $\sim 200$  K) the behavior is very similar to that of the grain, while for  $T \leq 180$  K the data display a significant kink: the magnetoresistive response can be divided in two contributions, the low-field magnetoresistance (LFMR) and the high-field magnetoresistance (HFMR). The more pronounced resistance drop appears at low field (LFMR), while the slope is smaller at higher fields (HFMR). With decreasing temperature, the LFMR effect increases, the HFMR slope decreases, and the field separating both regimes (hereafter denoted by  $H^*$ ) increases (Fig. 7 inset). This  $H^*$  field turns out to correspond to the saturation field of the bigrain, as determined by magnetic moment versus field measurements (Fig. 7).

We will first deal with the low field magnetoresistance. Although it is now generally accepted that LFMR is a grain boundary-related feature, the underlying physical mechanisms are still under debate. In a recent paper, Gupta and Sun<sup>26</sup> review the three main models: the spin-polarized tunneling (SPT) of charge carriers,<sup>27</sup> the spin-dependent scattering of polarized electrons,<sup>28,29</sup> and the mesoscopic model of Evetts *et al.*<sup>18</sup> This latter model supposes that the grain boundary region is polarized by adjacent magnetically soft grains and seems to be appropriate in our case, since the temperature dependence of  $H^*$  suggests that the saturation field  $H^*$  is directly related to the demagnetizing field. As the applied field is increased from zero to  $H^*$ , the ferromagnetic domains become progressively aligned and finally the bulk magnetization reaches the saturation value. This phenomenon can be at the origin of a grain boundary-related magnetoresistance. Indeed, as a charge carrier crosses the grain boundary, it undergoes a local change of the potential. If both grains are ferromagnetically aligned, the resulting magnetization creates an additional local magnetic field that promotes the order in the grain boundary and reduces the difference in potential encountered by the charge carrier. This mechanism is more efficient when the temperature is decreased, since the saturation magnetization is higher.

The high field magnetoresistive effect takes place at fields where the grain magnetization is already saturated. The high field allows the spins in the grain boundary to align, improving the conductivity of the material but without noticeable effect on the overall magnetization. Since the spin disorder decreases as the temperature decreases, the HFMR effect weakens when the temperature is reduced. Indeed the slope of the resistance versus magnetic field curve above  $H^*$  decreases with decreasing temperature. The especially large HFMR effect at 160 and 180 K can be explained by the fact that those temperatures coincide with the transition of the grain boundary material, where the application of a magnetic field is particularly efficient. The LFMR and HFMR effects appear to have opposite temperature dependences.

It is of interest to compare the above results to those obtained in thin films single boundaries and polycrystalline materials, which both exhibit a kink in the magnetoresistance at some given field  $H^*$ .<sup>11,15,18</sup> In thin films single boundaries, the  $H^*$  field roughly corresponds to the coercive field of the adjacent grains,<sup>18</sup> whereas in ceramics,  $H^*$  is linked to the saturation field,<sup>11</sup> as it is the case for the single boundaries in bulk materials presented in this article. Therefore the single boundaries in bulk materials and thin films do not behave in a similar manner. This is confirmed by examining the hysteresis of the  $R(H)$  curves: in thin films single boundaries, the hysteresis only concerns the LFMR,<sup>15,23</sup> while in our case a very small hysteresis, 20 mT, can be observed throughout the whole magnetic field range and temperature investigated.

#### IV. CONCLUSION

We have examined the electrical transport and magnetic properties of a bigrain sample extracted from a rod grown by the floating zone method. Resistance measurements carried out both within a grain and across the grain boundary show that the grain boundary has a strong influence on the transport properties. A foot-like feature can be observed towards the bottom of the transition. Besides, the residual low temperature resistance is two orders of magnitude higher than within the grain.

A huge magnetoresistance effect (up to 99%) was observed inside the grain. On the other hand, it turns out that (i) very high grain-boundary-related magnetoresistance values can be achieved under high magnetic field and (ii) grain boundary magnetoresistance is not only a low-field effect.

LFMR and HFMR effects have been studied at several temperatures. These behaviors have been analyzed within the framework of existing phenomenological models, in particular Evetts' mesoscopic model.

Finally our results for a single grain boundary in a bulk material have been compared to results for bicrystal thin films and polycrystalline materials. Noticeable differences have been pointed out.

#### ACKNOWLEDGMENTS

B. V. and Ph. V. thank F. N. R. S. (Fonds National de la Recherche Scientifique—Belgium) for research grants. Part of this work was carried out in the framework of the OXide

Spin Electronics Network (OXSEN) supported by the TMR program of the European Union. B. V. would like to express her thanks to Professor Revcolevski and Professor Berthet for kindly welcoming her at the Laboratoire de Physico-Chimie de l'Etat Solide.

- <sup>1</sup>J. M. D. Coey, M. Viret, and S. von Molnar, *Adv. Phys.* **48**, 167 (1999).
- <sup>2</sup>E. O. Wollan and W. C. Koehler, *Phys. Rev.* **100**, 545 (1955).
- <sup>3</sup>G. H. Jonker and J. H. Van Santen, *Physics* **XVI**, 337 (1950).
- <sup>4</sup>S. Jin, T. H. Tiefel, M. McCormack, R. A. Fastnacht, R. Ramesh, and L. H. Chen, *Science* **264**, 413 (1994).
- <sup>5</sup>C. N. R. Rao, A. K. Cheetham, and R. Manesh, *Chem. Mater.* **8**, 2421 (1996).
- <sup>6</sup>C. Zener, *Phys. Rev.* **82**, 403 (1951).
- <sup>7</sup>C. S. Hong, W. S. Kim, E. O. Chi, K. W. Lee, and N. H. Hur, *Chem. Mater.* **12**, 3509 (2000).
- <sup>8</sup>M. Sahana, M. S. Hegde, C. Shivakumara, V. Prasad, and S. V. Subramanyam, *J. Solid State Chem.* **148**, 342 (1999).
- <sup>9</sup>G. J. Snyder, R. Hiskes, S. DiCarolis, M. R. Beasley, and T. H. Geballe, *Phys. Rev. B* **53**, 14434 (1996).
- <sup>10</sup>L. E. Hueso, F. Rivadulla, R. D. Sanchez, D. Caeiro, C. Jardon, C. Vazquez-Vazquez, J. Rivas, and M. A. Lopez-Quintela, *J. Magn. Magn. Mater.* **189**, 321 (1998).
- <sup>11</sup>A. K. M. Akther Hossain, L. F. Cohen, F. Damay, A. Berenov, J. MacManus-Driscoll, N. McN. Alford, N. D. Mathur, M. G. Blamire, and J. E. Evetts, *J. Magn. Magn. Mater.* **192**, 263 (1999).
- <sup>12</sup>L. Balcells, B. Martinez, F. Sandiumenge, and J. Fontcuberta, *J. Magn. Magn. Mater.* **211**, 193 (2000).
- <sup>13</sup>W. Westerburg, F. Martin, S. Friedrich, M. Maier, and G. Jakob, *J. Appl. Phys.* **86**, 2173 (1999).
- <sup>14</sup>C. Höfener, J. B. Philipp, J. Klein, L. Alff, A. Marx, B. Büchner, and R. Gross, *Europhys. Lett.* **50**, 681 (2000).
- <sup>15</sup>K. Steenbeck, T. Eick, K. Kirsch, K. O'Donnel, and E. Steinbeiß, *Appl. Phys. Lett.* **71**, 968 (1997).
- <sup>16</sup>K. Steenbeck, T. Eick, K. Kirsch, H. G. Schmidt, and E. Steinbeiß, *Appl. Phys. Lett.* **73**, 2506 (1998).
- <sup>17</sup>N. D. Mathur, G. Burnell, S. P. Isaac, T. J. Jackson, B. S. Teo, J. L. MacManus-Driscoll, L. F. Cohen, J. E. Evetts, and M. G. Blamire, *Nature (London)* **387**, 266 (1997).
- <sup>18</sup>J. E. Evetts, M. G. Blamire, N. D. Mathur, S. P. Isaac, B. S. Teo, L. F. Cohen, and J. L. MacManus-Driscoll, *Philos. Trans. R. Soc. London, Ser. A* **356**, 1593 (1998).
- <sup>19</sup>Y. A. Soh, G. Aeppli, N. D. Mathur, and M. G. Blamire, *Phys. Rev. B* **63**, 020402(R) (2001).
- <sup>20</sup>K. A. Thomas, P. S. I. P. N. de Silva, L. F. Cohen, A. K. M. Akther Hossain, M. Rajeswari, T. Venkatesan, R. Hiskes, and J. L. MacManus-Driscoll, *J. Appl. Phys.* **84**, 3939 (1998).
- <sup>21</sup>D. Shulyatev, S. Karabashev, A. Arsenov, and Y. Mukovskii, *J. Cryst. Growth* **198/199**, 511 (1999).
- <sup>22</sup>A. de Andres, M. Garcia-Hernandez, and J. L. Martinez, *Phys. Rev. B* **60**, 7328 (1999).
- <sup>23</sup>S. P. Isaac, N. D. Mathur, J. E. Evetts, and M. G. Blamire, *Appl. Phys. Lett.* **72**, 2038 (1998).
- <sup>24</sup>J. Inoue and S. Maekawa, *Phys. Rev. Lett.* **74**, 3407 (1995).
- <sup>25</sup>N. Furukawa, *J. Phys. Soc. Jpn.* **64**, 2734 (1995).
- <sup>26</sup>A. Gupta and J. Z. Sun, *J. Magn. Magn. Mater.* **200**, 24 (1999).
- <sup>27</sup>N. Zhang, W. Ding, and W. Zhong, *Phys. Lett. A* **253**, 113 (1999).
- <sup>28</sup>A. Gupta, G. Q. Gong, G. Xiao, P. R. Duncombe, P. Lecoeur, P. Trouiloud, Y. Y. Wang, V. P. Dravid, and J. Z. Sun, *Phys. Rev. B* **54**, R15629 (1996).
- <sup>29</sup>X. W. Li, A. Gupta, G. Xiao, and G. Q. Gong, *Appl. Phys. Lett.* **71**, 1124 (1997).